Conical Beam Monopole Antenna Design for Chinese Area Positioning System

Feng Pang[1, 2], Guoxiang Ai[1], Jungang Yin[3], Yue Ma[1], Chao Hu[1], Junxia Cui[1], Lihua Ma[1], Chan Hwang See[4, 5], and Raed A. Abd-Alhameed[4, *]

Abstract—This article describes the operational principle of the satellite-based Chinese Area Positioning System (CAPS) and proposes a monopole antenna for a large anchored buoy platform in harshmarine environment. The proposed antenna is highly omnidirectional with sufficiently wide half-power beamwidth (HPBW) greater than 40° (i.e., not less than ±20° swing) by using a conical ground plane, taking into account the geostationary satellite position, link budget, sea conditions, volume and cost. The impedance bandwidth defined by 10 dB return loss is 750 MHz (5.60–6.35 GHz), and the main lobe direction and the half-power beamwidth are about 46° and 43° at the operating frequency 5.885 GHz, respectively. The antenna prototype has been installed on-site to test its performance in sea. The results confirm that the proposed antenna is a suitable candidate for a variety of CAPS applications in China.

1. INTRODUCTION

Oceanic buoys have for decades been applied to maritime hydrological and meteorological observations. Since most of the buoys work in harsh environment far away from the coastlines, conventional radio links or mobile systems can hardly satisfy the stringent specifications. The buoy platforms are thus widely used in a number of satellite-based navigation and telecommunication systems, such as GPS, ARGO and Inmarsat-C [1–3].

Chinese Area Positioning System (CAPS) takes advantage of communication satellites on the geostationary orbit (GEO) which uses transponders for both navigation and telecommunication functionalities. As for the maritime CAPS monitoring system, it consists of the GEO satellites, earth stations, user centers and large anchored oceanic buoys. A series of sensors are installed on the buoy platform, which is capable of automatically connecting data of the maritime environment, location and status of the buoy body before sending them to an earth station via GEO satellites. The earth station can process the received data and forward them to the user centers, while sending necessary control messages to the buoy on the other way around. The operational principle of the CAPS experimental system is illustrated in Fig. 1.
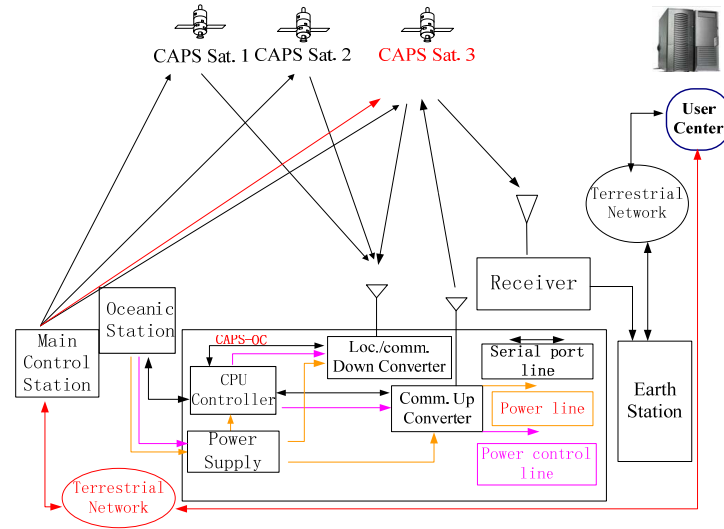
The CAPS Satellite 3 in Fig. 1 is on the Slightly Inclined Geostationary-Satellite Orbit (SIGSO) and mainly used as a transponder in the maritime monitoring system. Such an SIGSO satellite can improve positioning accuracy of CAPS and provide operation economy for telecommunications. SIGSO satellite is turned from decommissioned geosynchronous earth orbit satellite and only needs longitudinal station-keeping. Research shows that (i) SIGSO satellite inclination at a rate varying from year to year between 0.75°–0.95° [4], (ii) it will never exceed the natural limit of 14.5° in 18.6 years and (iii) then
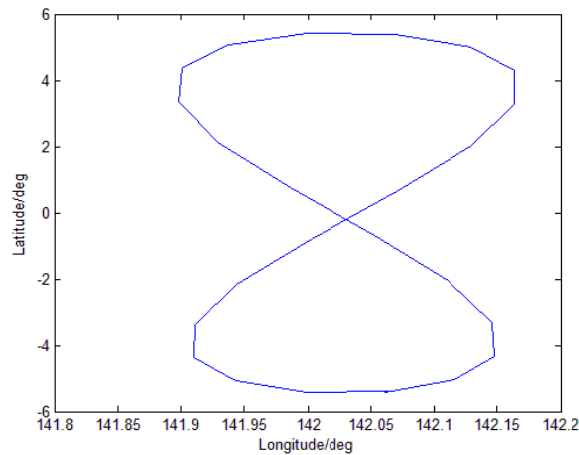
Figure 1. Operational principle of the CAPS experimental system.

Figure 2. Track of sub CAPS satellite 3.

decreases gradually at a cycle with a ground shaped as "8" [5, 6]. Fig. 2 is the track of sub CAPS Satellite 3 point whose inclination is $5.4°$. In order to track SIGSO satellite, buoy antenna pattern must be wide enough to accommodate the inclination changes. In addition, the buoy platform is subjected to waves, wind and corrosion due to the seawater. As a key component of the anchored buoy platform, the antenna should therefore be well qualified in terms of high-performance, high-reliability, low-profile and low-cost.

Circularly polarized conical beam antennas have been well adopted in the low G/T mobile satellite communication or the low/medium bit-rate satellite broadcasting services [7, 8], and short-range wireless communications [9, 10] in which maximum gain achieved between 4 dB and 6 dB over HPBW elevation angle varied from $\pm 40°$ to $\pm 50°$ with axial ratio less than 4 dB. However, these antennas are quite large and complicated in antenna geometry; therefore, they are not suitable for CAPS monitoring system. A monopole antenna is omnidirectional and commonly used in FM broadcasting, VHF/UHF communications, space and military applications since it has simple structure and capable of producing designable conical radiation patterns. It is also advantageous for the cost reduction as there is no need for tracking the satellites due to its omnidirectional patterns in the azimuth plane. A conventional monopole antenna consists of a straight rod-shaped radiator on a flat ground plane. It can be developed

into a wideband or multiband antenna through varying the shape of the radiator or implementing the loading techniques [11–13]. The performance can also be further improved by changing the shape or characteristics of the antenna ground plane. Ground planes in modified solid shape [14–16] or in defected shape [17] can be adopted to realize multiple resonances. In addition, using fractal [18] or quasi-fractal [19] ground plane in multiband monopole antennas can reduce the size of the antenna and enhance the performance. Recently, the artificial surface technology, including electrical bandgap (EBG) [20] and band-notch structures [21] can also be used in the ground plane of ultra-wideband monopoles for bandwidth enhancement and resonance flexibility.

However, from [11–21], it was found that no paper describes the design of a conical beam monopole antenna on an oceanic buoy platform. Particularly, of greater importance are to pointing the elevation angle over a wide beamwidth of the main lobe in the proposed application. In this article, a monopole antenna with conical ground plane is designed for the maritime CAPS monitoring system, where omnidirectional radiation patterns are required with half-power beamwidth (HPBW) greater than $40°$ and main lobe directing $46°$ relative to the zenith axis, according to the satellite link budget.

2. ANALYSIS AND SIMULATION

The dipole model together with the image theory is typically used to illustrate how the monopole fundamentally works. For monopoles with a finite-sized ground, the uniform theory of diffraction(UTD) can be incorporated with the ray-tracing technique to make an analytical solution to the radiation pattern [22, 23]. In this work, the commercial solver *CST MWS* was used to perform the modeling and antenna geometry parametric study.

The quarter wavelength monopole on a sufficiently large planar ground is the most common type of the conventional monopole antennas;its ideal model does not have any sidelobe, but the main lobe directs to the horizon (perpendicularly to the zenith axis). The three-quarter wavelength monopole otherwise does have side lobe, while its main lobe directs some certain angle relative to the horizon. The five-quarter wavelength monopole have higher gain, however, it has more sidelobes and the HPBW tends to be inadequate for the aimed swing range of $\pm20°$. Consequently, the three-quarter wavelength monopole was thus chosen as a good starting point for the design.

The geometry of the proposed omnidirectional monopole antenna is shown in Fig. 3, where L is the length of the rod conductor, D the diameter of bottom face, d the diameter of the upper face, and β the side angle.

(a)   (b)
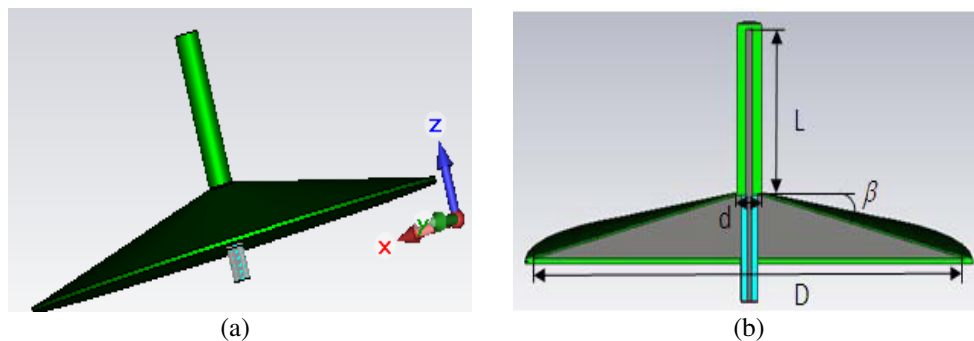
Figure 3. Geometry of the conical ground plane monopole antenna; (a) 3-D view, (b) center cut side view.

The conical ground works for modifying the elevation angle and HPBW of the main lobe. The rod radiator is fed by a coaxial cable reaching through the bottom of the ground plane. The performance was investigated at the center frequency 5.885 GHz by tuning the parameters L, β and D. A full parametric study was performed on the antenna elements to achieve certain performances of such antenna in terms return loss (S_{11}, as shown in Figs. 4 to 6) and radiation patterns as shown in Figs. 7 to 9.

The initial length of the rod radiator L is $0.75\lambda_0$ as mentioned above, and it becomes shorter when the radiator is covered by a dielectric housing ($\varepsilon_r = 2.2$) for the purpose of packaging and anti-corrosion.
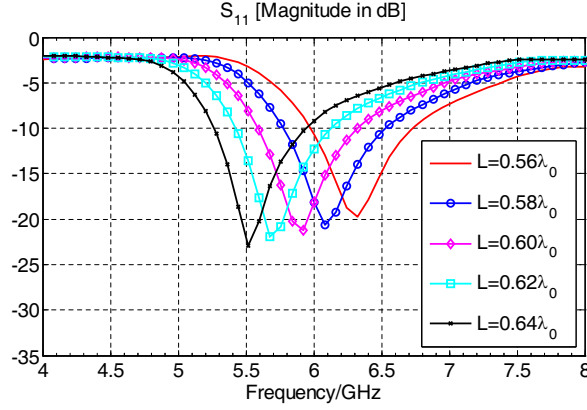
Figure 4. Parameter L sweep for S_{11} (other parameters are set as in Table 1).
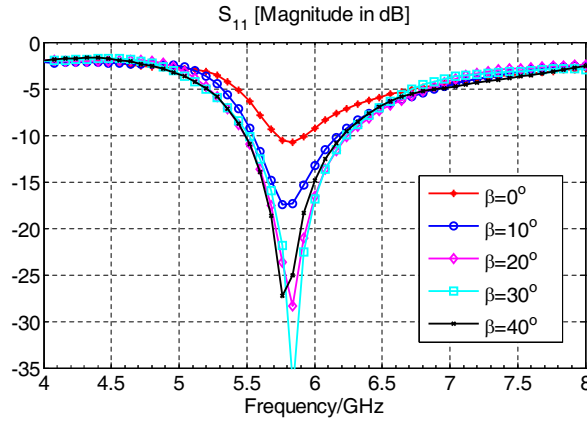

Figure 5. Parameter β sweep for S_{11} (other parameters are set as in Table 1).
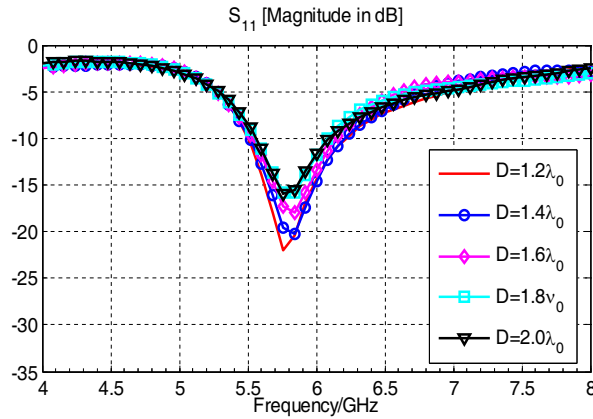

Figure 6. Parameter D sweep for S_{11} (other parameters are set as in Table 1).

L is the most sensitive factor for variation of the resonance points, but insensitive for the change of the radiation patterns. Therefore, L is optimized in the first place.

As opposed to L, the side angle β is otherwise the most sensitive factor for both the direction and HPBW of the main lobe, while very little variation of the resonance points is observed when it is changed. However, there exists some difference in the deepness of the tips in the sweep of β.

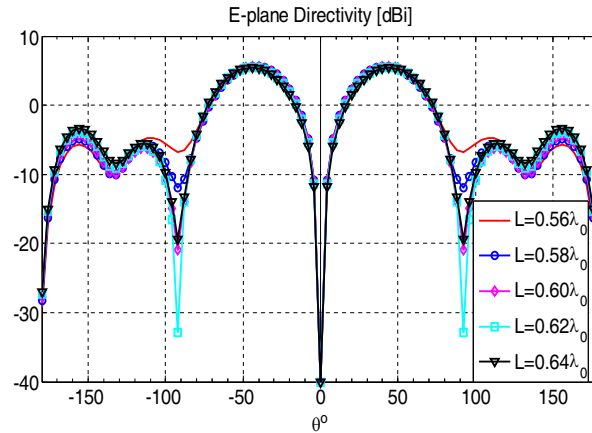The bottom diameter D does not change much either in resonance tips or in the main lobe directions,

Figure 7. Parameter L sweep for patterns (other parameters are set as in Table 1).
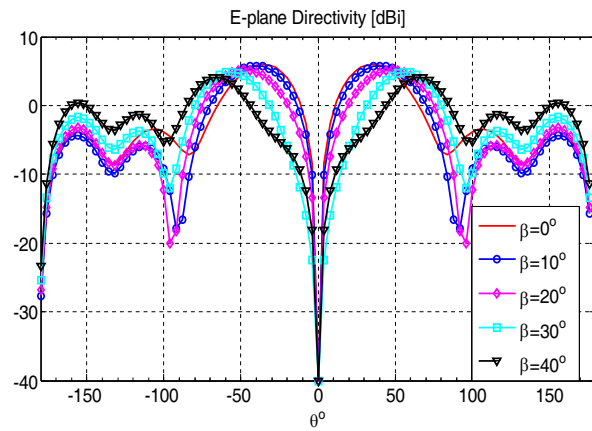

Figure 8. Parameter β sweep for patterns (other parameters are set as in Table 1).
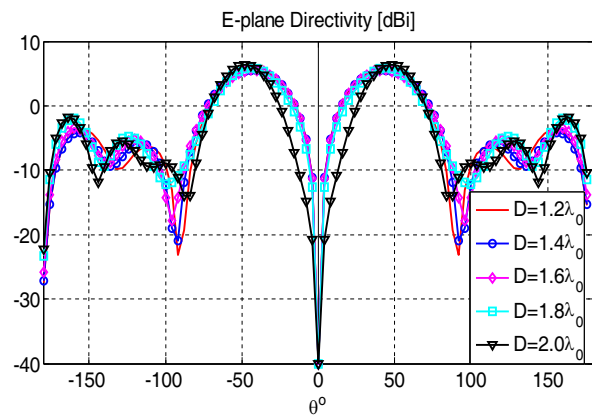

Figure 9. Parameter D sweep for patterns (other parameters are set as in Table 1).

and it can thus be used to fine-tune the HPBW. It should be sufficiently large in terms of λ_0 (wavelength at center frequency of the operating band) for a desired beamwidth; meanwhile, it has to be as small as possible in view of the volume, weight and cost. The trade-off was made based on plenty of parameter sweep simulations.

The top diameter d is made small enough just for supporting the rod radiator and found to be

of minor importance. The dimensions of the optimized monopole antenna are given in Table 1, where the operating frequency is 5.885 GHz, corresponding to a wavelength of about 51 mm in free space. By the way, this antenna is installed on the top of a quite large anchored buoy platform and more than 10 meters above the sea level, so the influence on the radiation patterns by the seawater can be neglected.

**Table 1.** Dimensions of the dielectric-housed monopole antenna.

| D	L	β	d	λ_0
$1.3\lambda_0$	$0.61\lambda_0$	$14°$	$6\,\text{mm}$	$51\,\text{mm}$

3. MEASURED RESULTS

The S_{11} of the antenna was measured by an Agilent N5230C network analyzer. The radiation pattern and antenna gain were measured inside anechoic chamber. The measured S_{11} and copolar radiation pattern are shown in Figs. 10 and 11, respectively. It can be seen that the 10 dB impedance bandwidth has been covered between 5.60 and 6.35 GHz (i.e., a total bandwidth of 750 MHz that is equivalent to 12.5% relative bandwidth), and the resonance point is deviated by 25 MHz from the original operating center frequency 5.885 GHz; including an error around 100 MHz was found between simulated and measured resonant frequencies, due to some mechanical tolerances. The main beam angle is around 46° relative to the zenith axis and the HPBW is about 43° at 5.885 GHz. The measured maximum antenna
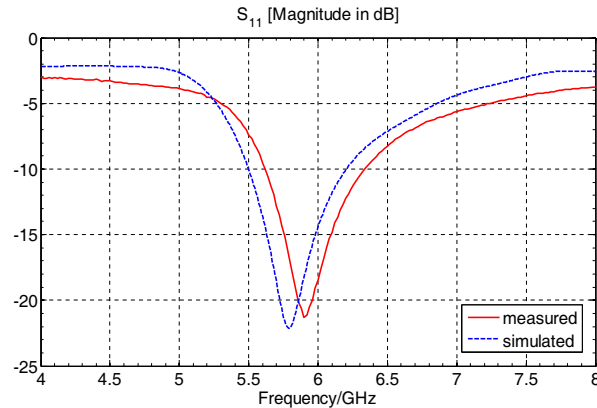
Figure 10. The measured magnitude of S_{11} of the monopole antenna.
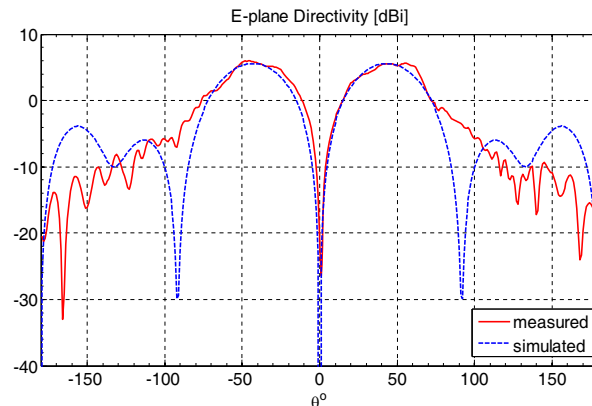
Figure 11. The measured directivity of the manufactured antenna at 5.885 GHz.
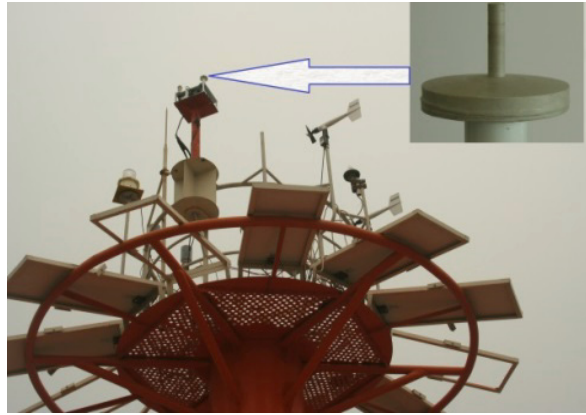
Figure 12. The antenna installed on the top of the oceanic buoy platform.

gain is about 5.7 dB that is quite satisfactory towards the required limit of the link budget for such system application. The measured patterns generally agree well with the simulation results, though the measured far-out/back lobes are somewhat lower.

As pictured in Fig. 12, the antenna was installed on the top of an oceanic buoy platform in China East Sea. It was about 10 meters high above the sea level, and the influence on radiation patterns from the sea surface and other objects was found negligible. The system had survived a series of functional tests for 15 days in a row, when even very tough conditions (maximum wave height 4.8 m, maximum wind speed 12.2 m/s) occurred in sea. During the on-site tests, data capture rate up to 100% and bit error rate better than 10^6 of the navigation/communication system were recorded.

4. CONCLUSIONS

In this paper, we propose a C-band buoy monopole antenna with a conical ground plane that is used to adjust the main lobe direction and the beamwidth to satisfy the satellite link requirements when installed on an oceanic buoy platform. Different side angles were studied before the dimensions were optimized finally. The measurement results show that its 10 dB impedance bandwidth ranges from around 5.60 to 6.35 GHz; the main lobe direction and HPBW are about 46° and 43° at 5.885 GHz, respectively. The measurement results agree well with the simulation ones. The on-site tests of the monopole antenna were performed in sea and turned out to succeed in meeting the system requirements. The proposed buoy antenna has been finalized for use in the maritime CAPS monitoring system in China.

ACKNOWLEDGMENT

REFERENCES

1. Niu, H.-N. and P. Li, "The implementation of inmarsat-C/GPS technology in buoy system," *Journal of China Institute of Communications*, Vol. 22, No. 5, 67–70, 2001.

2. Zhang, R.-H., J. Zhu, J.-P. Xu, Y.-M. Liu, Q.-Q. Li, and T. Niu, "Argo global ocean data assimilation and its applications in short-term climate prediction and oceanic analysis," *Chinese Journal of Atmospheric Sciences*, Vol. 37, No. 2, 411–424, 2013.

3. Zhang, S.-Y., Y. Lin, and X.-Y. Chi, "Study on argos transmitter terminal and its applications," *Ocean Technology*, Vol. 24, No. 1, 25–28, 2005.

4. International Telecommunication Union, "Recommendation ITU-R S.484-3. Station-keeping in longitude of geo-stationary satellites in the fixed-satellite service," International Telecommunication Union Electronic Publishing Service, Geneva, 2004.

5. Shi, H. L., G. X. Ai, Y. B. Han, et al., "Multi-life cycles utilization of retired satellites," *Sci. China Ser. G-Phys. Mech. Astron.*, Vol. 52. No. 3, 323–327, 2009.

6. International Telecommunication Union, "Recommendation ITU-R S.743-1, The coordination between satellite networks using slightly inclined geostationary-satellite orbits (GSOs) and between such networks and satellite networks using non-inclined GSO satellites," International Telecommunication Union Electronic Publishing Service, Geneva, 2004.

7. Wang, Z., et al., "An inmarsat BGAN terminal patch antenna array with unequal input impedance elements and conductor-backed ACPW series-feed network," *IEEE Transactions on Antennas and Propagation*, Vol. 60, No. 3, 1642–1647, 2012.

8. Wang, L., et al., "Design of a new printed dipole antenna using in high latitudes for inmarsat," *IEEE Antennas and Wireless Propagation Letters*, Vol. 10, 2011.

9. McEwen, L. N. J., R. A. Abd-Alhameed, E. M. Ibrahim, P. S. Excell, and N. T. Ali, "Compact WLAN disc antennas," *IEEE Transactions on Antennas and Propagation*, Vol. 50, No. 12, 1862–1864, 2002.

10. Zhou, D., R. A. Abd-Alhameed, C. H. See, and P. S. Excell, "New circularly-polarised conical-beam microstrip patch antenna array for short-range communication systems," *Microwave and Optical Technology Letters*, Vol. 51, 78–81, Jan. 2009

11. Su, S. W., K. L. Wong, and C. L. Tang, "Ultra-wideband square planar monopole antenna for IEEE 802.16a operation in the 2–11 GHz band," *Microwave and Optical Tech. Letters*, Vol. 32, No. 4, 463–466, 2004.

12. Zhang, F. F., et al., "Design and investigation of broadband monopole antenna loaded with non-foster circuit," *Progress In Electromagnetics Research C*, Vol. 17, 254–255, 2010.

13. Kim, J.-Y., N. Kim, S. Lee, and B.-C. Oh, "Triple band-notched UWB monopole antenna with two resonator structures," *Microwave and Optical Technology Letters*, Vol. 55, No. 1, 4–6, 2013.

14. Go, H.-C. and Y.-W. Jang, "Multi-band modified fork-shaped microstrip monopole antenna with ground plane including dual-triangle portion," *Electronics Letters*, Vol. 40, No. 10, 2004.

15. Chawanonphithak, Y. and C. Phongcharoenpanich, "Miniaturized dual-band π-shaped monopole antennas with modified rectangular ground plane," *Proc. of 11th International Conference on Electrical Engineering Electronics, Computer, Telecommunications and Information Technology, ECTI-CON*, 2014.

16. Shah, S. A. A., M. F. Khan, S. Ullah, and J. A. Flint, "Design of a multi-band frequency reconfigurable planar monopole antenna using truncated ground plane for Wi-Fi, WLAN and WiMAX applications," *International Conf. on Open Source Systems and Technologies*, 2014.

17. Antoniades, M. A. and G. V. Eleftheriades, "A compact multiband monopole antenna with a defected ground plane," *IEEE Antennas and Wireless Propagation Letters*, Vol. 7, 2008.

18. Gemio, J., J. P. Granados, and J. S. Castany, "Dual-band antenna with fractal-based ground plane for WLAN applications," *IEEE Antennas and Wireless Propagation Letters*, Vol. 8, 2009.

19. Hong, T., S.-X. Gong, Y. Liu, and W. Jiang, "Monopole antenna with quasi-fractal slotted ground plane for dual-band applications," *IEEE Antennas and Wireless Propagation Letters*, Vol. 9, 2010.

20. Elsheakh, D. N., H. A. Elsadek, E. A. Abdallah, H. Elhenawy, and M. F. Iskander, "Enhancement of microstrip monopole antenna bandwidth by using EBG structures," *IEEE Antennas and Wireless Propagation Letters*, Vol. 8, 2009.

21. Aghdam, S. A. and S. M. H. Varkiani, "Small monopole antenna with semicircular ground plane for UWB applications with variable band-notch structure," *Microwave and Optical Technology Letters*, Vol. 55, No. 1, 12–14, 2013.

22. Keller, J. B., "Geometrical theory of diffraction," *J. Opt. Soc. Am.*, Vol. 52, No. 2, 116–130, 1962.

23. Kouyoumjian, R. G. and P. H. Pathak, "A uniform geometrical theory of diffraction for an edge in a perfectly conducting surface," *Proc. IEEE*, Vol. 62, 1448–1461, November 1974.